Tumor cytokine profile of renal cell carcinoma patients

Moon Hee Lee
University of Helsinki, Helsinki University Hospital Comprehensive Cancer Center
Essi Laajala
University of Helsinki, Helsinki University Hospital Comprehensive Cancer Center
Anna Kreutzman
University of Helsinki, Helsinki University Hospital Comprehensive Cancer Center
Petrus Järvinen
Helsinki University and Helsinki University Hospital
Harry Nísen
Helsinki University and Helsinki University Hospital
Tuomas Mirtti
Helsinki University Hospital, University of Helsinki
Maija Hollmén
University of Turku
Satu Mustjoki (satu.mustjoki@helsinki.fi)
University of Helsinki, Helsinki University Hospital Comprehensive Cancer Center

Research Article

Keywords: renal cell carcinoma, cytokines, chemokines, biomarkers, tumor immunology

Posted Date: March 7th, 2022

DOI: https://doi.org/10.21203/rs.3.rs-1415222/v1

Abstract

Purpose

Renal cell carcinoma (RCC) accounts for 90% of all renal cancers and is considered highly immunogenic. Although many studies have reported the circulating peripheral cytokine profiles, the signatures between the tumor tissue and matching healthy adjacent renal tissue counterparts have not been explored. We aimed to comprehensively investigate the cytokine landscape of RCC tumors and its correlation between the amount and phenotype of the tumor infiltrating lymphocytes (TILs).

Experimental Design

We analyzed the secretion of 42 cytokines from the tumor (n=50) and adjacent healthy kidney tissues (n=24) with a Luminex-based assay. We further explored the differences between the tissue types, as well as correlated the findings with clinical data and detailed immunophenotyping of the TILs.

Results

Using an unsupervised clustering approach, we observed distinct differences in the cytokine profiles between the tumor and adjacent renal tissue samples. The tumor samples clustered into three distinct profiles based on the cytokine expressions: high (53.2% of the tumors), intermediate (25.5%), and low (21.3%). Most of the tumor cytokines positively correlated with each other, except for IL-8 that showed no correlation with any of the measured cytokine expressions. Furthermore, the quantity of lymphocytes in the tumor samples analyzed with flow cytometry positively correlated with the chemokine-family of cytokines, IP-10 and MIG. Positive correlations were also observed between CD4+, CD8+ T cell PD-1 expressions and IL-8, suggesting a suppressive role of the chemotactic cytokine, even in T cell inflamed tumors.

Conclusions

Our study highlights the distinct cytokine profiles in RCC and provides insights to potential biomarkers for the treatment of RCC.

Introduction

Renal cell carcinoma (RCC) is a heterogeneous cancer that accounts for more than 90% of cancers in the kidney, with the clear cell (ccRCC) subtype as the major cause of kidney cancer-related deaths[1]. Although radical nephrectomy remains the gold standard surgical treatment, approximately 30% of patients with ccRCC with localized disease develop metastases[2–5]. As a tumor that is resistant to radiation and chemotherapy, RCC is also known to be a highly angiogenic, vascularized cancer that expresses VEGF and is counterintuitively characterized by heavy lymphocytic infiltration compared to other solid tumors[6,7].

Cytokines are essential signaling molecules that elicit an immune response. In addition to regulating host responses to infections, cytokines are also involved in inflammation and dysregulation of the immune system in cancer, diabetes, and viral infections[8,9]. In many solid tumors including RCC, tumor cells acquire various cytokines and their corresponding receptors from the surrounding normal stroma to grow, proliferate, and survive[9,10]. Although previous studies have analyzed the circulating cytokines in the blood[11,12], comparisons between the cytokines released from the tumor and matching adjacent healthy renal tissue have not been fully explored.

Our recent data showed immunological differences between RCC tumors that displayed T and NK cell dominant immune phenotypes[13]. In this study, we aimed to explore the underlying cytokine signatures that are present within the tumor environment compared to the adjacent healthy renal tissue, and in turn, correlate the profiles with the immunophenotype and clinical data.

Materials And Methods

Patients and study approval

The study included newly diagnosed RCC (n=43) and non-RCC (n=7) patients that underwent radical nephrectomy (Supplemental Table S1). The primary tumor and the adjacent healthy renal tissue samples were obtained from the patients during the surgical procedures within a four-year time frame.

Non-RCC cases such as rectal carcinoma (n=1), urothelial carcinoma (n=1) and benign RCC angiomyolipoma (n=1) were excluded from all analyses. The study was approved by the Helsinki University Hospital ethical committee (Dnro 115/13/03/02/15) and was conducted in accordance with the Declaration of Helsinki. All patient samples were taken after a signed informed consent.

Sample preparation and processing

A prospective sample collection of freshly excised tumor and matching adjacent healthy tissue samples were collected (2016-2020) and stored in MACS® tissue storage solution (Miltenyi Biotec 130-100-008) at 4°C upon harvest. All samples were processed directly upon arrival at our facilities within minimal transportation time. Each sample was independently dissociated using Miltenyi's Tumor Dissociation kit protocol (Miltenyi Biotec 130-095-929). A portion of the freshly dissociated cells were viably frozen in 10% FBS-DMSO solution and preserved at -150°C for the cytokine assay.

Clinical data

An assessment of 18 clinical parameters (tumor size and weight, TNM staging, WHO/ISUP 2016 tumor grading simplified into two classes: low (G1-G2) and high (G3-G4), presence of necrosis, peri-renal and peri-pelvic fat infiltration, rhabdoid histology, age at relapse) and other medical histories were included (Supplemental Table S1).

Conditioned media

Conditioned media were obtained from each dissociated tumor (n=50) and adjacent healthy renal tissue (n=24) sample. First, 100 000 cells in 150mL/well were seeded in 96-U well culture plates and cultured in tumor cell media (RPMI-1640, 10% FBS, 1% Penicillin/Streptomycin, 2mM L-Glutamine, 10mM sodium pyruvate, hydrocortisone sodium succinate (Solu-Cortef) 0.0004mg/mL) for 24h at 37°C, 5% CO_2. The next day, cells were washed twice with PBS to remove any remaining serum, replaced with unsupplemented RPMI-1640, and were incubated for 24h at 37°C, 5% CO_2. The conditioned media were collected and filtered through a 0.2mm syringe before use. Details of the conditioned media protocol have previously been described in detail[14,15].

Multiplex cytokine assay

The presence of various cytokines such as chemokines, growth factors, and interleukins (pg/mL) from the serum-free conditioned media were analyzed using the Bio-Plex Pro™ human cytokine screening panel (Bio-Rad) according to the manufacturer's instructions.

Statistical analyses

I. Tumor-Healthy comparisons

Non-parametric Mann-Whitney U-test (unpaired, two-tailed) with a 95% confidence level was used to compare two groups. All scatter dot plots show error bars with the median and range as horizontal lines. The statistical analyses were performed using Prism 9 Version 9.2.0 (GraphPad Software Inc.). For all graphs: ns, not significant; *, p<0.05; **, p<0.01; ***, p<0.001; ****, p<0.0001.

II. Heatmap and correlation analyses

Unsupervised heatmap clustering was carried out by using the Euclidean distance and ward.D2 linkage method after $\log_2$ transforming and Z-score scaling the data. The Z-score scaling was performed for each cytokine (row). Spearman's correlation and hierarchical clustering with the complete linkage method were used for the correlation plot (Fig. 2), which was created with the R package, corrplot[16]. R version 4.0.4.[17], RStudio version 1.3.1056 and the Python package CytoMod[18] were used for the analyses. Benjamini and Hochberg-corrected p-values with a false discovery rate (FDR) < 0.05 with were considered significant.

Results

RCC tumors display a distinct cytokine profile compared to the healthy renal tissue counterparts

First, we assessed the cytokine landscape of the RCC tumors in comparison to the profiles of the adjacent healthy renal tissue samples. Our cohort included 50 tumor cases, out of which 36 (72%) were ccRCC, 4

(8%) chromophobe RCC, 3 (6%) papillary RCC, and 4 (8%) benign oncocytoma cases, confirmed by histopathological analysis (Table 1). Angiomyolipoma, rectal carcinoma and urothelial carcinoma cases were excluded from all analyses. From a total of 47 tumor cases, we randomly selected 24 matching healthy renal tissue samples that were histopathologically confirmed.

Table 1
Sample cohort and patient characteristics

Patients	**All (n = 50)**
Tumor	50
Matching adjacent healthy renal tissue	24
Age in years: mean (range)	66 (23–85)
Sex: n (%)	
Male	28 (56)
Female	22 (44)
Tumor histology: n (%)	
Clear cell	36 (72)
Chromophobe	4 (8)
Papillary	3 (6)
Oncocytoma (benign)	4 (8)
Angiomyolipoma*	1 (2)
Rectal carcinoma*	1 (2)
Urothelial Carcinoma*	1 (2)
WHO/ISUP 2016 tumor grade at diagnosis: n (%)	
I-II	25 (50)
III-IV	20 (40)
Unknown	5 (10)
Deaths due to metastasis: n (%)	
Yes	2 (4)
No	48 (96)
* Excluded from the analysis	

Using an unsupervised approach, we analyzed the cytokine profiles of the tumor and healthy tissues (Fig. 1A). Our heatmap analysis showed that the samples were divided into two main clusters: samples with high cytokine expressions and those with low expressions. Seven out of 31 samples (23%) in the highly expressing group were healthy tissue samples, compared to 17/40 samples (42%) in the lowly expressing cytokine group. Furthermore, all the tumor tissue samples in the highly expressing group clustered together with the matching healthy tissues (except for patient 28, an oncocytoma case). In the lowly expressing cytokine cluster, seven paired healthy-tumor samples belonged to the same group, whereas in nine healthy cases, the corresponding tumor samples belonged to the highly expressing cluster, and one healthy tissue case lacked a matching tumor sample.

Next, we compared in detail the cytokine profiles between the tumor and healthy adjacent renal tissues and discovered significant differences between the samples in 22 out of a total of 42 measured cytokines. Overall, the cytokine levels in the tumor (T) tissues were greater compared to the healthy (H) counterparts, except in FGF, where a moderate increase in concentration was observed in the healthy tissue than in the tumor samples (Fig. 1B-D). The biggest differences between the tumor-healthy samples were detected in the interleukin and chemokine ligand concentrations: IL-1α ($p < 0.0001$, median 5.4pg/mL vs 2.6pg/mL), IL-2Ra ($p < 0.0001$, median 12.5pg/mL vs 7.1pg/mL), IL-18 ($p < 0.0001$, median 3.2pg/mL vs 0.9pg/mL) (Fig. 1B); IP-10 (CXCL10) ($p = 0.0042$, median 2.0pg/mL vs 1.1pg/mL) and MIG (CXCL9) ($p < 0.0001$, median 50.6pg/mL vs 6.5pg/mL) (Fig. 1C). Additionally, the expression of growth factors such as VEGF were increased in the tumor samples compared to the healthy tissues (Fig. 1D). A full comparison of the tumor and healthy cytokines are found in the Supplemental Fig. S1A-E.

Intratumoral cytokines highly correlate with each other

To better understand the individual differences in the patient samples, we independently analyzed the cytokine profiles in the tumor samples using the same unsupervised approach and observed three main clusters: tumors with high (hi), intermediate (int), and low (lo) cytokine expressions (Fig. 2A). 25 out of 47 (53.2%) tumor cases belonged to the hi group, whereas 12 (25.5%) and 10 (21.3%) samples belonged to the cytokine int and lo groups, respectively. No differences were found in the clinical parameters such as gender, age, WHO ISUP 2016 tumor grading, and presence of necrosis between the clusters. Similarly, although tumors were divided into distinct subgroups based on the immune profiles (CD3 + T and NK cell dominant) from our previous study[13] (Supplemental Fig. S2A), and PD-1 high (PD1_hi) and low (PD1_lo) expression based on the CD4 + and CD8 + T cell PD-1 expression (Supplemental Fig. S2B), the subgroups were evenly distributed among the cytokine profiles.

Subsequently, using Spearman's rank correlation and a false discovery rate (FDR) < 0.05 across the tumor cytokines, we discovered strong positive correlations across the majority of the expressed cytokines (Fig. 2B), suggesting that tumors expressing high levels of a particular cytokine were likely to exhibit increased expression signatures of the other cytokines as well. One of the highest positive correlations was found between IL-6 and IL-9 (Fig. 2C). Contrarily, IL-3, PDGF-BB, VEGF, β-NGF, and SCGF-β showed positive correlations with only a handful of cytokines, making their expression profiles different from the rest. IL-8 displayed no correlation with any of the measured cytokines and was lowly expressed in a

proportion of the samples that belonged to the cytokine hi cluster (Fig. 2A, B, D). Apoptosis-related cytokines such as TRAIL, TNF-β and IFN-γ were among the top cytokines that exhibited the highest correlations, whereas IL-8 displayed a negative correlation between the overall mean tumor cytokine levels (Fig. 2D). Furthermore, using the same unsupervised hierarchical clustering methods, we analyzed the cytokine profiles of the healthy adjacent renal tissues (n = 24). Similarly, the healthy tissue samples clustered into three clusters based on the cytokine expressions (hi, int, and lo) (Supplemental Fig. S3A). As observed with the tumor tissues, most of the cytokines in the healthy tissues positively correlated with each other in their expression profiles, except for IL-8. (Supplemental Fig. S2A, B).

The expression of IP-10 and MIG are correlated with tumor lymphocyte abundance

We next sought to investigate whether certain cytokines would impact the immune cell infiltration in the tumor. Although the tumor cytokine profiles did not cluster based on the CD3 + T and NK cell dominant immunophenotypes (Fig. 2A), we analyzed the cytokine profiles in relation to the quantity and phenotype of the TILs. The total amount of TILs in tumor samples did not significantly differ between the hi and lo cytokine tumor groups (Supplemental Fig. S2C). However, when individual cytokines were examined, IP-10, MIG, IL-16 and IL-1Ra expressions significantly correlated with lymphocyte abundance (Fig. 3Ai-iv). We further analyzed the quantity of CD3 + T and NK cells out of all cells in the tumor samples and observed that IP-10, IL-16, and IL-1Ra levels were significantly correlated with the number of tumor infiltrating CD3 + T cells (Fig. 3Bi-iii), with the strongest correlation between MIG (Fig. 3Biv). The expression of IP-10 also correlated with tumor infiltrating NK cells, whereas no correlations between MIG, IL-16, IL-1Ra and NK cell count were found (Supplemental Fig. S4Ai-iii). In accordance, MIG levels were significantly higher in the CD3 + T cell dominant tumors compared to NK cell dominant tumors ($p = 0.005$) (Fig. 3C). Although elevated IP-10, IL-16 and IL-1Ra expressions were increased in the CD3 + T cell dominant tumors compared to the NK dominant counterparts, no statistical differences were observed (Supplemental Fig. S4Bi-iii).

CD4 + and CD8 + T cell PD-1 tumor immunophenotypes positively correlate with IL-8, whereas VEGF levels correlate with CXCR4, DNAM and CD57 expressions in specific T cell subgroups

Because IL-8 expression showed no correlation with the rest of the measured cytokines, we further investigated its relationship with the immune phenotype of the tumors. We found significant positive correlations between IL-8 and PD-1 expressions in CD4+ ($p = 0.007$, $r = 0.39$) and CD8+ ($p = 0.03$, $r = 0.32$) T cells (Fig. 4A, B). We were also interested in the expression profile of VEGF, a key extracellular growth factor known to stimulate angiogenesis in RCC. As a result, we identified a positive correlation between VEGF and the expression of the chemokine receptor CXCR4 in CD4 + T cells ($p = 0.0008$, $r = 0.50$), but not in CD8 + T cells ($p = 0.074$, $r = 0.27$) (Fig. 4C, D). Additionally, VEGF levels negatively correlated with CD8 + T cell DNAM ($p = 0.01$, $r=-0.36$) and CD4 + T cell CD57 ($p = 0.01$, $r=-0.36$) expressions. Among the other chemokines, CXCR3 expression in the CD4 + T, CD8 + T and NK cells displayed strong negative

correlations with several interleukins such as IL-4, IL-5, IL-6, IL-9, and IL-10, as well as with IFN-γ, TNF-β, and TRAIL (Supplemental Fig. S2C).

Discussion

In this study, we measured 42 cytokines from RCC tumors together with the matching adjacent renal tissues, to investigate the cytokine profiles and correlate the findings with the immunophenotype of the TILs and clinical parameters. Our results show that the cytokine profiles found in the tumor are distinct from the healthy counterparts. However, we observed that tumors with high cytokine expression signatures also have increased cytokine levels in the matching adjacent healthy tissues. Most of the cytokines showed significantly positive correlations with each other in their expression levels, suggesting that cytokine-enriched tumors have an overall inflamed tumor microenvironment.

Although previous studies have analyzed the circulating cytokines in RCC[11,12,19] and in other solid tumors[20–22] from serum or plasma samples, our work describes the cytokine profile in the actual tumor microenvironment.

While the proportion of the TILs did not significantly differ between the cytokine highly and lowly expressing tumors, IP-10 (CXCL10) and MIG (CXCL9), known to belong to the CXC chemokine subfamily were associated with increased lymphocyte quantities in the tumor samples. The MIG-CXCR3 axis is mainly known to regulate cell migration activation and immune reactivity through the recruitment of activated T cells, NK cells and NKT cells[23]. Similarly, IP-10 is released in response to IFN-γ, and is a chemotactic factor involved in the recruitment of activated T and NK cells to sites of inflammation[20]. Our results suggest that both cytokines are involved in the recruitment and homing of T and NK cells into the tumor microenvironment in RCC. Unfortunately, our previous immunophenotyping analysis[13] did not include markers for macrophages or other immune cells in addition to the lymphocytes. Therefore, tumors with a highly expressing cytokine profile most likely have increased quantities of other immune cells, such as those in the myeloid compartment that contribute to the immune inflamed tumor microenvironment.

The clinically relevant marker, PD-1, expressed on CD4 + T and CD8 + T cells showed positive correlations with IL-8 levels, a cytokine that did not correlate with any other cytokine. IL-8, also known as CXCL8, is known to be a proinflammatory cytokine involved in the recruitment of immune cells and tumor progression via epithelial-to-mesenchymal transition[24]. Recent studies by Yuen et al have shown that high baseline plasma IL-8 or on-treatment increased IL-8 levels correlated with an overall decreased survival and response rate to anti-PD-L1 therapy in patients with metastatic urothelial carcinoma and metastatic RCC[19]. Other studies have also shown that increased intratumoral IL-8 expression correlates with high levels of immune suppressive myeloid cells, such as neutrophils and monocytes[25,26]. Based on our data, the baseline tumor IL-8 expression does not correlate with metastasis formation, and the follow-up is too short to reveal whether the cytokine has an impact on the overall survival.

In our cohort, the CXCR4 expression in the CD4 + T cells correlated with VEGF levels in the tumor tissue. Previous studies have shown that CXCR4 expression is upregulated by HIF-1α activation as well as VEGF[21] not only for gliomas, but also in RCC, due to mutations from the von Hippel-Lindau tumor suppressor (*VHL*) gene responsible for hypoxia. It is thought that together with VEGF, CXCR4 drives angiogenesis and metastasis by activating numerous signaling pathways. Furthermore, chemokine receptors such as CXCR4 are known to facilitate the migration of regulatory T cells into the tumors by their corresponding ligands in the tumor microenvironment.

In conclusion, our study highlights the cytokine profile in relation to the TILs in treatment naïve RCC samples. Further work including single cell analysis and functional studies are needed to provide a comprehensive understanding of cytokine signaling in the inflamed tumor microenvironment and the impact of individual cytokines in RCC.

Declarations

Funding

details

Contributions

Conception and design: MHL, SM. Collection and assembly of clinical data: PJ, MHL, TM, HN. Collection and assembly of data: PJ, MH, MHL. Data analysis: EL, MHL. Data interpretation: all authors. Manuscript writing: MHL, EL, SM. Editing and final approval of manuscript: all authors.

Acknowledgements

The authors sincerely thank the patients who donated the samples used in the study. All physicians and technicians involved in patient enrolment and sample procurement are thanked for their efforts. We also heartily thank the members of Hematology Research Unit Helsinki for their advice and technical support. We thank Teija Kanasuo for carrying out the multiplex cytokine assay.

References

1. Hsieh JJ, Purdue MP, Signoretti S, et al. Renal cell carcinoma. Nat Rev Dis Primers. Mar 9 2017;3:17009. doi:10.1038/nrdp.2017.9
2. Frank I, Blute ML, Cheville JC, Lohse CM, Weaver AL, Zincke H. An outcome prediction model for patients with clear cell renal cell carcinoma treated with radical nephrectomy based on tumor stage, size, grade and necrosis: the SSIGN score. J Urol. Dec 2002;168(6):2395–400. doi:10.1097/01.ju.0000035885.91935.d5

3. Patard JJ, Kim HL, Lam JS, et al. Use of the University of California Los Angeles integrated staging system to predict survival in renal cell carcinoma: an international multicenter study. J Clin Oncol. Aug 15 2004;22(16):3316–22. doi:10.1200/JCO.2004.09.104
4. Wolff I, May M, Hoschke B, et al. Do we need new high-risk criteria for surgically treated renal cancer patients to improve the outcome of future clinical trials in the adjuvant setting? Results of a comprehensive analysis based on the multicenter CORONA database. Eur J Surg Oncol. May 2016;42(5):744–50. doi:10.1016/j.ejso.2016.01.009
5. Meskawi M, Sun M, Trinh QD, et al. A review of integrated staging systems for renal cell carcinoma. Eur Urol. Aug 2012;62(2):303–14. doi:10.1016/j.eururo.2012.04.049
6. Jubb AM. Expression of vascular endothelial growth factor, hypoxia inducible factor 1, and carbonic anhydrase IX in human tumours. *Journal of Clinical Pathology*. 2004-05-01 2004;57(5):504–512. doi:10.1136/jcp.2003.012963
7. Khan KA, Kerbel RS. Improving immunotherapy outcomes with anti-angiogenic treatments and vice versa. *Nature Reviews Clinical Oncology*. 2018-05-01 2018;15(5):310–324. doi:10.1038/nrclinonc.2018.9
8. Furman D, Campisi J, Verdin E, et al. Chronic inflammation in the etiology of disease across the life span. Nature Medicine. 2019-12-01 2019;25(12):1822–1832. doi:10.1038/s41591-019-0675-0
9. Dranoff G. Cytokines in cancer pathogenesis and cancer therapy. *Nature Reviews Cancer*. 2004-01-01 2004;4(1):11–22. doi:10.1038/nrc1252
10. Hinshaw DC, Shevde LA. The Tumor Microenvironment Innately Modulates Cancer Progression. *Cancer Research*. 2019-09-15 2019;79(18):4557–4566. doi:10.1158/0008-5472.can-18-3962
11. Chehrazi-Raffle A, Meza L, Alcantara M, et al. Circulating cytokines associated with clinical response to systemic therapy in metastatic renal cell carcinoma. *Journal for ImmunoTherapy of Cancer*. 2021-03-01 2021;9(3):e002009. doi:10.1136/jitc-2020-002009
12. Guida M, Casamassima A, Monticelli G, Quaranta M, Colucci G. Basal cytokines profile in metastatic renal cell carcinoma patients treated with subcutaneous IL-2-based therapy compared with that of healthy donors. *Journal of Translational Medicine*. 2007-12-01 2007;5(1):51. doi:10.1186/1479-5876-5-51
13. Lee MH, Jarvinen P, Nisen H, et al. T and NK cell abundance defines two distinct subgroups of renal cell carcinoma. Oncoimmunology. 2022;11(1):1993042. doi:10.1080/2162402X.2021.1993042
14. Hollmén M, Roudnicky F, Karaman S, Detmar M. Characterization of macrophage - cancer cell crosstalk in estrogen receptor positive and triple-negative breast cancer. Scientific Reports. 2015-08-01 2015;5(1):9188. doi:10.1038/srep09188
15. Hollmén M, Karaman S, Schwager S, et al. G-CSF regulates macrophage phenotype and associates with poor overall survival in human triple-negative breast cancer. OncoImmunology. 2016-03-03 2016;5(3):e1115177. doi:10.1080/2162402x.2015.1115177
16. Simko TWV. R package 'corrplot': Visualization of a Correlation Matrix (Version 0.91). 2021;

17. Team RC. R: A language and environment for statistical computing. R Foundation for Statistical Computing, Vienna, Austria. 2020;
18. Cohen L, Fiore-Gartland A, Randolph AG, et al. A Modular Cytokine Analysis Method Reveals Novel Associations With Clinical Phenotypes and Identifies Sets of Co-signaling Cytokines Across Influenza Natural Infection Cohorts and Healthy Controls. Front Immunol. 2019;10:1338. doi:10.3389/fimmu.2019.01338
19. Yuen KC, Liu L-F, Gupta V, et al. High systemic and tumor-associated IL-8 correlates with reduced clinical benefit of PD-L1 blockade. *Nature Medicine*. 2020-05-01 2020;26(5):693–698. doi:10.1038/s41591-020-0860-1
20. Tominaga M, Iwashita Y, Ohta M, et al. Antitumor effects of the MIG and IP-10 genes transferred with poly [D,L-2,4-diaminobutyric acid] on murine neuroblastoma. Cancer Gene Therapy. 2007-08-01 2007;14(8):696–705. doi:10.1038/sj.cgt.7701059
21. Zagzag D, Lukyanov Y, Lan L, et al. Hypoxia-inducible factor 1 and VEGF upregulate CXCR4 in glioblastoma: implications for angiogenesis and glioma cell invasion. *Laboratory Investigation*. 2006-12-01 2006;86(12):1221–1232. doi:10.1038/labinvest.3700482
22. Jabeen S, Espinoza JA, Torland LA, et al. Noninvasive profiling of serum cytokines in breast cancer patients and clinicopathological characteristics. OncoImmunology. 2019-02-01 2019;8(2):e1537691. doi:10.1080/2162402x.2018.1537691
23. Tokunaga R, Zhang W, Naseem M, et al. CXCL9, CXCL10, CXCL11/CXCR3 axis for immune activation – A target for novel cancer therapy. Cancer Treatment Reviews. 2018-02-01 2018;63:40–47. doi:10.1016/j.ctrv.2017.11.007
24. David J, Dominguez C, Hamilton D, Palena C. The IL-8/IL-8R Axis: A Double Agent in Tumor Immune Resistance. Vaccines. 2016-06-24 2016;4(3):22. doi:10.3390/vaccines4030022
25. Schalper KA, Carleton M, Zhou M, et al. Elevated serum interleukin-8 is associated with enhanced intratumor neutrophils and reduced clinical benefit of immune-checkpoint inhibitors. *Nature Medicine*. 2020-05-01 2020;26(5):688–692. doi:10.1038/s41591-020-0856-x
26. Bakouny Z, Choueiri TK. IL-8 and cancer prognosis on immunotherapy. *Nature Medicine*. 2020-05-01 2020;26(5):650–651. doi:10.1038/s41591-020-0873-9

Figures

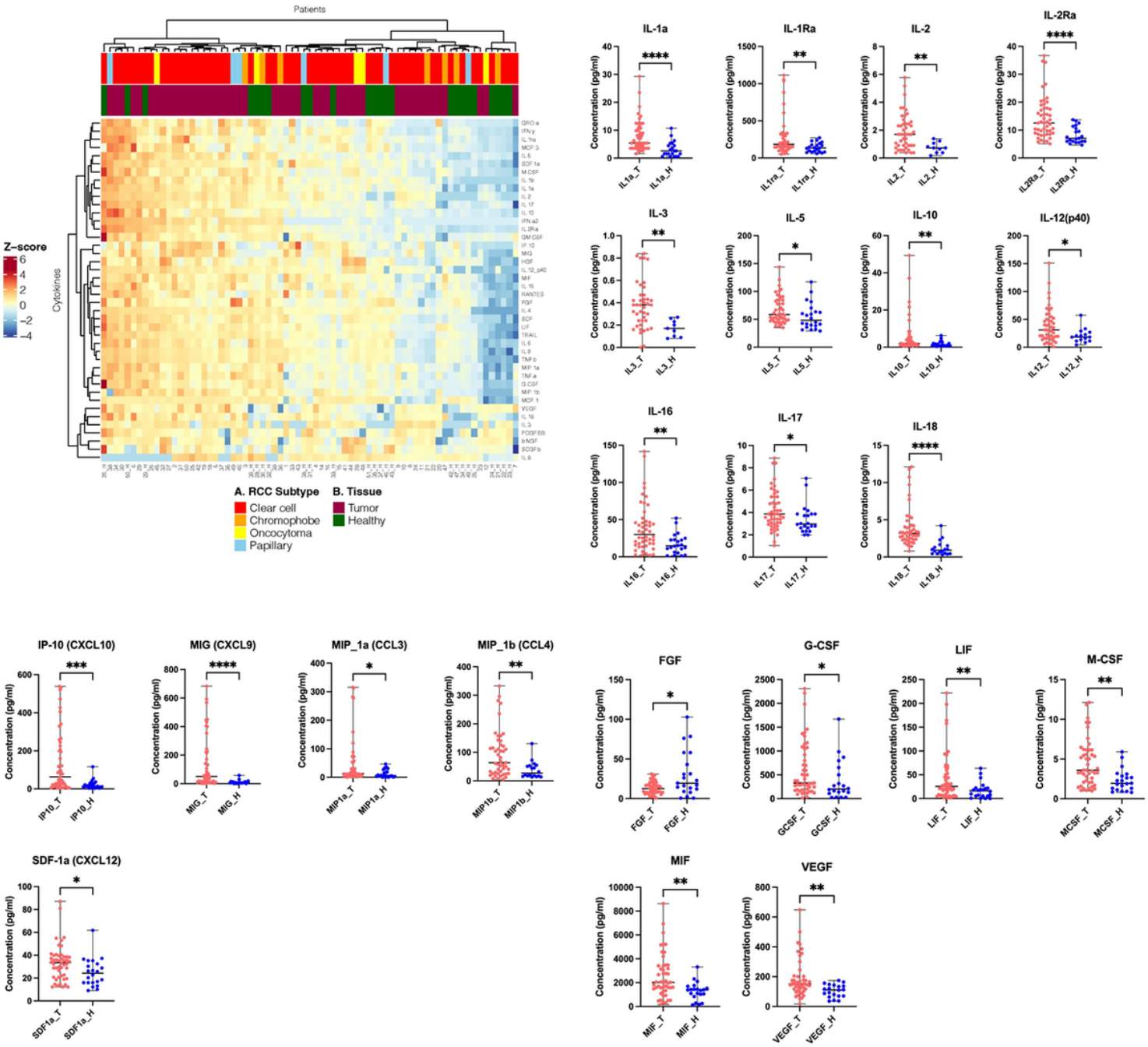

Figure 1

A. Heatmap showing the cytokine profile of RCC tumors (n=50) and healthy adjacent tissue samples (n=24) using unsupervised clustering. Upper color keys represent clinical parameters (RCC histology and type of tissue sample). Euclidean distance clustering and ward.D2 linkage methods were used from $\log_2$ transformed data values. Numerical identifiers at the bottom of the heatmap refer to individual patient tumors, where "_H" codes correspond to the healthy tissue counterparts. From the cytokine profiles, patients may be divided into two large clusters – those with high and those with low cytokine expression profiles.

B.–D. Comparison of each cytokine profile between the tumor and healthy adjacent renal tissue samples show significant differences, with the tumors generally displaying a higher expression and broader range of cytokines. The cytokines were grouped based on their biological qualities: (B) interleukin families, (C) chemokine ligands, (D) growth, inhibiting and stimulating factors. All other cytokines are found in the Supplemental Fig. S1A-E. Non-parametric Mann-Whitney U test was used with a 95% confidence level. Horizontal error bars indicate the median and range. *, p<0.05; **, p<0.01; ***, p<0.001; ****, p<0.000.1

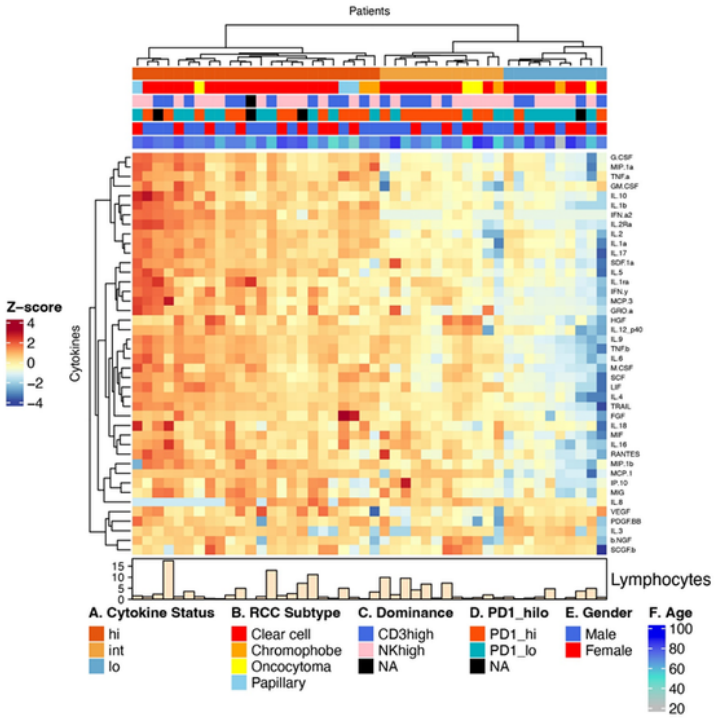

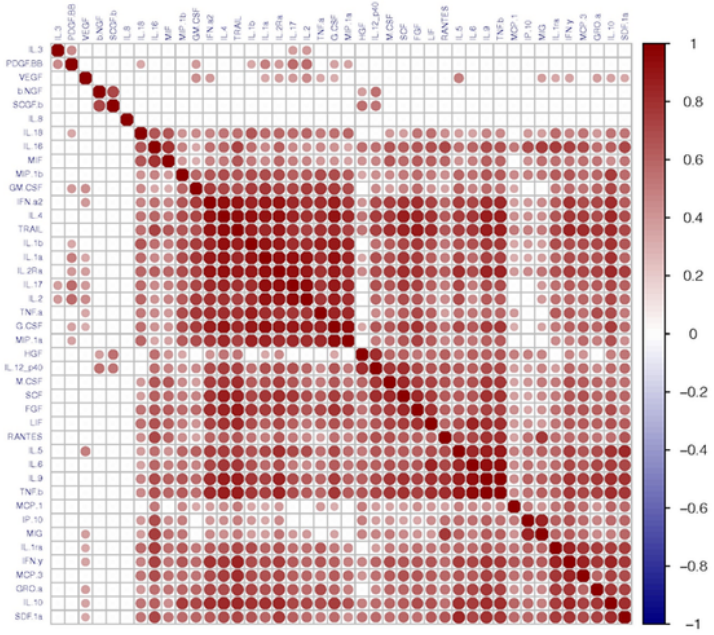

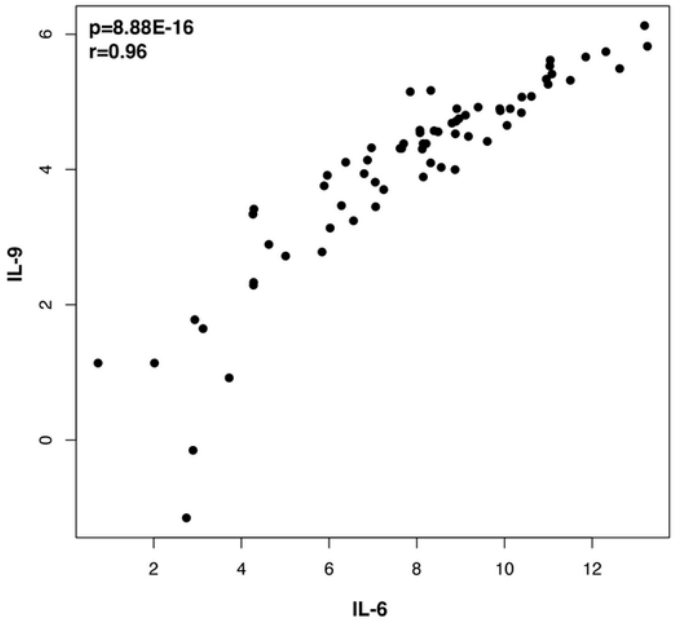

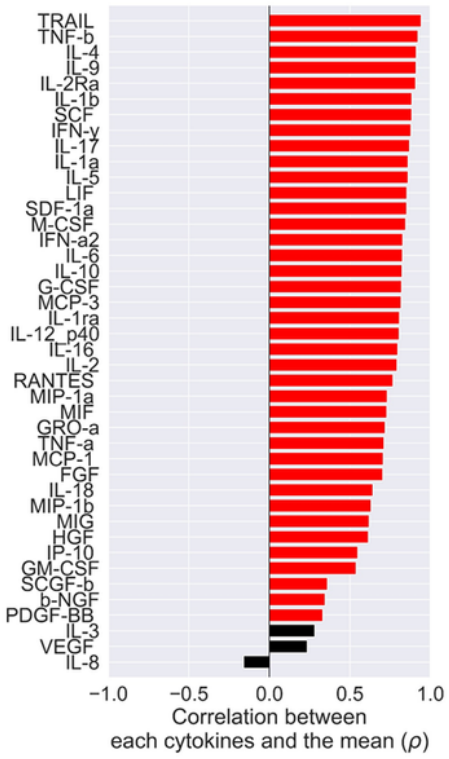

Figure 2

A. Heatmap of RCC tumors expressing a total of 42 cytokines, with clinical parameters such as the RCC subtype, gender, and age. Unsupervised Euclidean distance clustering and ward.D2 linkage methods were used. RCC tumors have a distinct cytokine profile based on three clusters ((A) Cytokine Status): those with high (hi), intermediate (int), and low (lo) cytokine expressions. No marked differences were observed between the clinical parameters. The (C) Dominance and (D) PD1_hilo color keys refer to our previous studies[13] with RCC tumors that were subgrouped into CD3+ T and NK cell dominant tumors (Supplemental Fig. S2A), or CD4+ and CD8+ T cell PD-1 expression (Supplemental Fig. S2B). NAs refer to samples excluded from the analysis or with missing clinical data.

B. Correlation plot using Spearman rank correlation shows strong positive correlations across most of the cytokines expressed in the tumor. However, different expression patterns were observed for a few cytokines (IL-3, PDGF-BB, VEGF, b-NGF, and SCGF-b). IL-8 was the only cytokine that showed no correlation with any of the measured cytokine levels. Only statistically significant cytokines (Bonferroni-Hochberg corrected) with a false discovery rate (FDR) < 0.05 are shown.

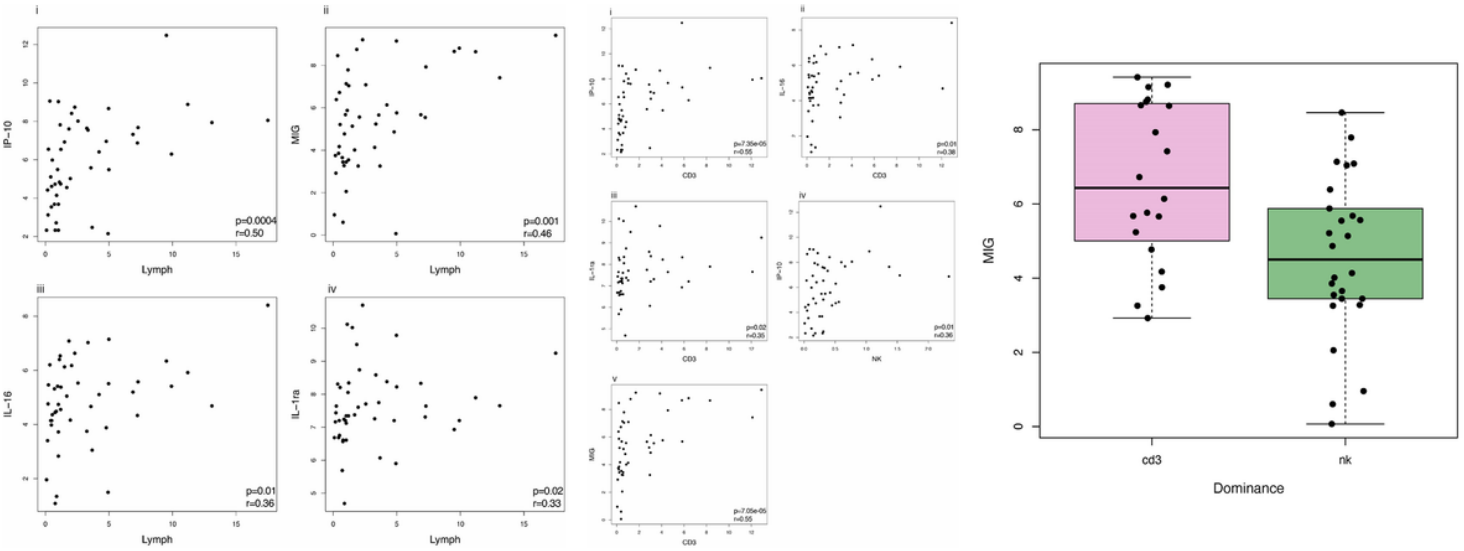

Figure 3

A. Scatterplots showing Spearman's correlation between the expression of various cytokines (IP-10, MIG, IL-16, and IL-1ra) with the overall quantity of lymphocytes in the tumor samples: (i) IP-10 vs Lymphocytes; (ii) MIG vs Lymphocytes; (iii) IL-16 vs Lymphocytes; (iv) IL-1ra vs Lymphocytes. Lymph = Lymphocytes. IP-10 and MIG showed the strongest positive correlations with the abundance of lymphocytes in the tumor. p = p-value, r = Spearman's rho.

B. Scatterplots showing Spearman's correlation between the expression of the cytokines and CD3+ T and NK cell abundance out of all cells in the tumor: (i) IP-10 vs CD3; (ii) IL-16 vs CD3; (iii) IL-1Ra vs CD3; (iv) MIG vs CD3; (v) IP-10 vs NK. MIG and CD3+ T cell abundance, as well as IP-10 and NK cell abundance showed the strongest positive correlations. p = p-value, r = Spearman's rho.

C. Boxplot showing the expression of MIG that was significantly elevated in the CD3+ T cell dominant compared to the NK cell dominant tumors (p=0.005).

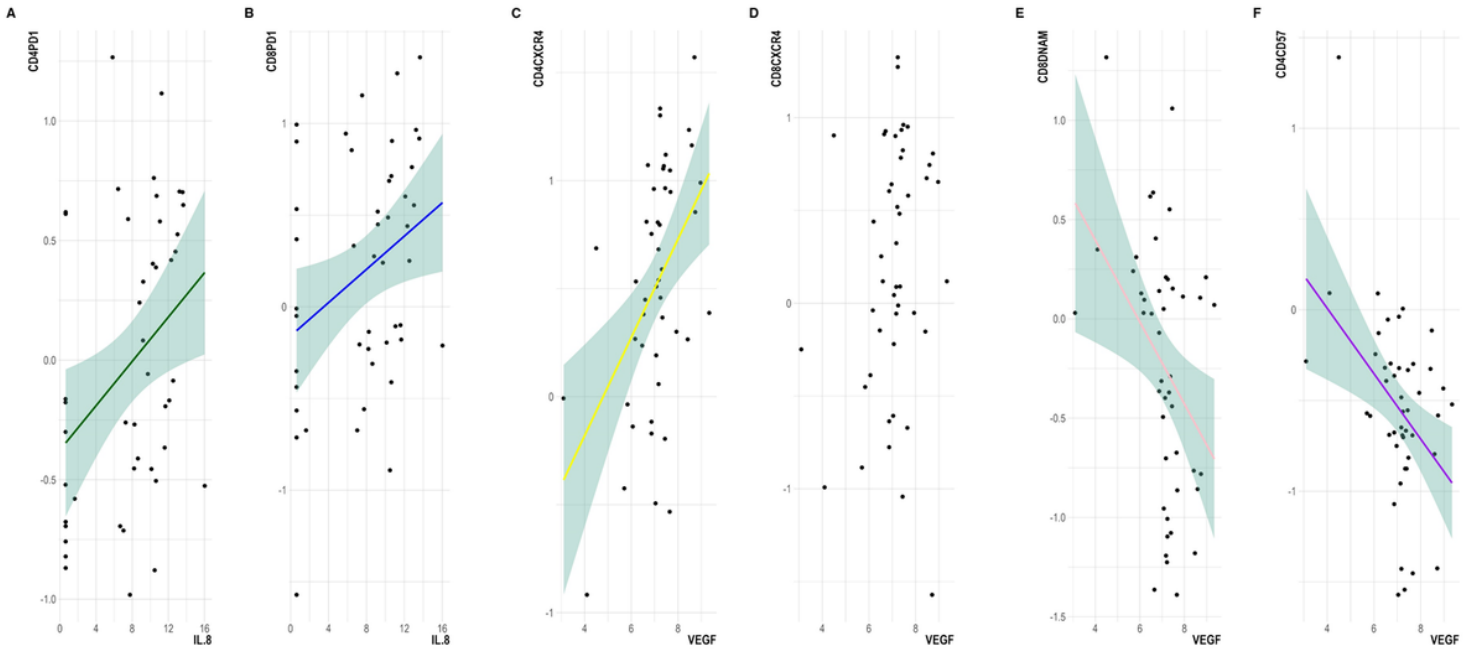

Figure 4

A. Scatterplot showing Spearman's correlation between CD4+ T cell PD-1 expression and IL-8 across all tumor samples (p=0.007, r=0.40). CD4+ T cell PD-1 expression showed a stronger correlation with IL-8 levels compared to the expression of PD-1 in CD8+ T cells.

B. Scatterplot showing Spearman's correlation between CD8+ T cell PD-1 expression and IL-8 concentration (p=0.03, r=0.32).

C. Scatterplot showing positive Spearman's correlation between CD4+ T cell CXCR4 expression and VEGF (p=0.0008, r=0.48).

D. No correlation was found between CD8+ T cell CXCR4 expression and VEGF levels (p=0.074, r=0.27).

E. Scatterplot showing negative Spearman's correlation between CD8+ T cell DNAM and VEGF expressions (p= 0.01, r=-0.36).

F. Scatterplot showing negative Spearman's correlation between CD4+ T cell CD57 expression and VEGF levels (p= 0.01, r=-0.36).

Supplementary Files

This is a list of supplementary files associated with this preprint. Click to download.

- suppfiglegends.docx
- supptables1.xlsx
- suppfigs.pptx